Mathematical and Computer Modelling 50 (2009) 1606–1621

Contents lists available at ScienceDirect

Mathematical and Computer Modelling

journal homepage: www.elsevier.com/locate/mcm

Expansion of high pressure gas into air — A more realistic blast wave model

Ejanul Haque [a], Philip Broadbridge [b,*], P.L. Sachdev [c]

[a] School of Mathematical & Geospatial Sciences, RMIT University, PO Box 2476V, Melbourne, Victoria 3001, Australia

[b] School of Engineering & Mathematical Sciences, La Trobe University, Victoria 3086, Australia

[c] Department of Mathematics, Indian Institute of Science, Bangalore, Karnataka 560 012, India

ARTICLE INFO

Article history:
Received 20 August 2009
Accepted 1 October 2009

Keywords:
Blast wave
Explosion
Shock wave
Gas dynamics
Compressible flow

ABSTRACT

In this paper, we consider a more realistic model of a spherical blast wave of moderate strength. An arbitrary number of terms for the series solution in each of the regions behind the main shock – the expansion region, the nearly uniform region outside the main expansion and the region between the contact surface and the main shock, have been generated and matched across the boundaries. We then study the convergence of the solution by using Padé approximation. It constitutes a genuine analytic solution for a moderately strong explosion, which, however, does not involve a secondary shock. The pressure distribution behind the shock however shows some significant changes in the location of the tail of the rarefaction and the interface, in comparison to the planar problem. The theory developed for the spherical blasts is also extended to cylindrical blasts. The results are compared with the numerical solution.

1. Introduction

Over the years, particularly during World War-II, there has been considerable interest in the theory of strong explosions, for example, those caused by nuclear devices [1–6]. Numerous attempts have been made to obtain analytical solutions for flow problems in non-stationary gas dynamics involving transition fronts such as shock waves, rarefaction waves and contact surfaces. Such fronts occur in shock tube flows, cylindrical and spherical explosions, implosions, combustion, deflagration and detonations. The vast majority of approximate analytic solution methods assume that either the disturbance is weak or the explosion obeys a given similarity constraint. The latter constraint is based on two assumptions: the explosion is intense so that the shock produced by it is of infinite strength. This helps the idealization that the energy of the explosion is released at a point. The second assumption is that the energy remains constant during the entire course of propagation of the blast. While this approximation holds very well in the early stages of a strong explosion, it begins to fail soon. Also, if the initial energy of the blast is not very large, this model is not appropriate.

The present problem is different from the point explosion. It concerns relatively weaker explosions. It may be stated as follows. A perfect idealized gas at high pressure is held stationary by a thin spherical diaphragm of unit radius, and is surrounded by a second perfect gas at uniform low pressure. Henceforth, the inner medium will be referred to as 'gas', and the outer medium as 'air'. At time $t = 0$, the diaphragm is destroyed and the gas rushes outward, compressing the air around it. The subsequent behavior may be described by a space–time diagram (see Fig. 1). Region A contains undisturbed gas. Region B contains the rarefaction wave bounded by its 'head', a straight characteristic on the left, and its 'tail', on the

* Corresponding author. Tel.: +61 03 94792107; fax: +61 03 94793060.
E-mail addresses: ejanul.haque@rmit.edu.au (E. Haque), P.Broadbridge@latrobe.edu.au (P. Broadbridge).

0895-7177/$ – see front matter © 2009 Elsevier Ltd. All rights reserved.
doi:10.1016/j.mcm.2009.10.002

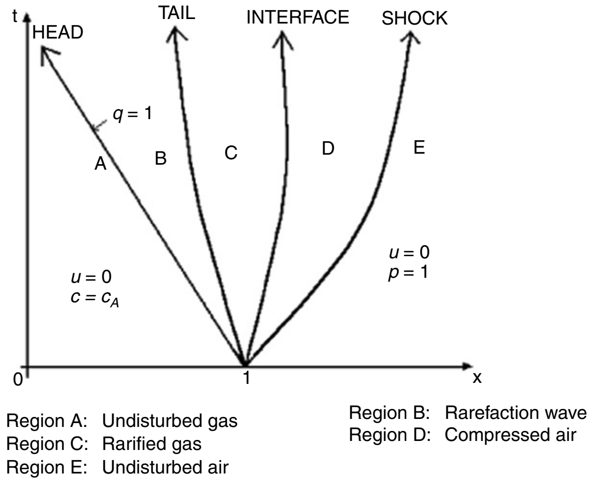

Fig. 1. Space–time distribution for a spherical blast.

right. The latter, another characteristic, adjoins region C. In this region the gas is rapidly expanding, irrespective of the behavior outside the tail. Region C consists of a rarefied fan moving outward. An interface or contact surface separates the gas from region D containing shock-compressed air moving outside. The interface is a contact discontinuity across which pressure and particle velocity are continuous but other variables get a jump. Region E is undisturbed air. The transition from region E to region D takes place via a shock. The gas sphere is not envisaged to be at a very high pressure; thus it is assumed that no secondary shock is formed. This phenomenon was subsequently discussed by Friedman [7].

One of the earliest attempts at modelling a blast wave – which was not too strong – was due to McFadden [8]. He carried out the analysis, which would provide him an initial solution to continue the computation of the problem by numerical methods, then available, without the need to tackle discontinuities in the initial data. He considered a unit sphere containing a perfect gas at uniformly high pressure instantaneously expanding into a homogeneous atmosphere. The particle velocity, sound speed, and entropy were developed in powers of y (the distance moved by the head of the rarefaction wave in time t), with coefficients depending on a slope coordinate q (see Section 3 for definition). While McFadden's was a good first attempt, he found the solution only up to two terms in the series. The zeroth order solution in the series is simply the solution of the shock tube problem. McFadden [8] found just the first order correction for various regions and showed how geometry affected the shock tube problem in the first order approximation. The solution is valid only for a very short time and can hardly be expected to give any accurate results for large time. Later, Yogi [9] had extended this problem by using a series solution method. However, the boundary conditions used by him for higher order ($n > 1$) terms are inappropriate. Indeed, the boundary conditions are very important to find the solutions in different regions and the unknown boundaries. A careful analysis of the series solutions and its convergence and computational efficacy remain to be investigated.

Haque [10] improvised and generalized this problem which was later discussed by Sachdev [11]. Haque [10] had given the analytic solution in each region explicitly for five terms in series; in powers of y. In this paper we discuss three terms explicitly and for higher order we refer to [10]. The coefficients become more difficult and cumbersome as the number of terms increase. The series solution with five terms in y converges for small time for spherical geometry, as shown in Table 2. Beyond this time, the convergence slows down, leading to inaccurate results.

We extend the series solution of the blast wave problem to make it reasonably valid for 'sufficiently large time' after the explosion. For this purpose we generate numerically a large number of coefficients in the series (3.2). We use both the direct sum and Padé approximation [12–16] to extend the validity of the series solution in time (see Table 4).

The analytic character of the series solution in region B changes for $\gamma = 5/3$ and $\gamma = 3$, the series becomes a psi series in $q \ln q$ and q (see Section 7).

2. Mathematical formulation

A perfect gas at high pressure is held stationary by a thin uniform diaphragm within a cylinder or a sphere of unit radius. It is surrounded by air at a uniformly low pressure. At time $t = 0$, the diaphragm is destroyed and the gas rushes outward compressing the air around it. The subsequent behavior of the expanding medium is described by space–time diagram shown in Fig. 1.

The spherical (or cylindrical) geometry introduces several difficulties. The spherical term in the equation of continuity prevents solution of the problem by the classical one-dimensional method; the tail of the rarefaction wave, the contact front, and the shock front travel with varying speeds; the entropy varies spatially in the air behind the shock front.

If p is the pressure, ρ the density, u the particle velocity, S the entropy per mole, x the radial distance from the geometric center and t the time, the Eulerian equations governing the planar, cylindrical and spherical symmetry ($\sigma = 0$, 1 and 2, respectively) flows are

$$\rho(u_t + uu_x) + p_x = 0, \tag{2.1}$$

$$\rho_t + u\rho_x + \rho(u_x + \sigma u/x) = 0, \tag{2.2}$$

$$S_t + uS_x = 0, \tag{2.3}$$

where the subscripts (t and x) denote differentiation. In addition to these equations we must consider the equation of state of perfect gas,

$$p\rho^{-\gamma} = \gamma^{-\gamma} \exp(S/c_v), \tag{2.4}$$

where $\gamma = c_p/c_v$, the ratio of specific heats. Note that although (2.3) is a conservation law, the solution has entropy increasing as the shock passes.

The spatial variable x and time t have been normalized by the initial blast radius x_0 and x_0/c_E, respectively; c_E is the speed of sound in the region E outside the blast wave. The radial velocity and sound speed have been rendered non-dimensional by c_E. Hence we have

$$u = \bar{u}/c_E, \qquad c = \bar{c}/c_E, \qquad x = \bar{x}/x_0, \quad t = \bar{t}c_E/x_0.$$

Barred quantities are the actual physical variables. A more suitable form of the equations of motion is obtained by expressing p and ρ in terms of S and the sound speed $c = (\gamma\ p/\rho)^{1/2}$ and by absorbing the constant in a new entropy function

$$s = S/c_v\gamma(\gamma - 1). \tag{2.5}$$

The flow variables p and ρ are now written as

$$p = c^{(\alpha+2)} \exp(-\gamma s), \qquad \rho = \gamma c^{\alpha} \exp(-\gamma s), \tag{2.6}$$

where $\alpha = (2N - 1)$ and $2N = (\gamma + 1)/(\gamma - 1)$.

Thus the new equations of motion are

$$u_t + uu_x + \alpha cc_x - c^2 s_x = 0, \tag{2.7}$$

$$\alpha(c_t + cc_x) + c(u_x + \sigma u/x) = 0, \tag{2.8}$$

$$s_t + us_x = 0. \tag{2.9}$$

The system (2.7)–(2.9) must be satisfied in each of the five regions A to E, shown in Fig. 1. The solutions are trivial in regions A and E. For $t = 0$, the (non-dimensional) initial conditions in the region A ($0 \le x \le 1$) are $u = 0, c = c_A$, and in the region E ($x > 1$) are $u = 0, c = 1, s = 0$ ($s = 0$ is actually normalized by subtracting from it some value $s = s_0$, say). For $t > 0$, the above conditions also prevail in regions A and E. The boundary conditions that must be satisfied in the intervening regions B, C and D for $t > 0$ are described as follows.

The head of the rarefaction wave,

$$x_H = 1 - c_A t, \tag{2.10}$$

is a characteristic and permits a jump in the derivatives of u, c, and s across it; the functions u, c, and s must however be continuous. Thus, when $x = x_H$, we have the conditions

$$u_B = 0, \qquad c_B = c_A, \qquad s_B = s_A, \tag{2.11}$$

under the restriction that the rarefaction wave has not yet reached the center i.e. $0 < t < 1/c_A$.

The tail of the rarefaction wave is assumed to be a characteristic moving inward, at a variable speed relative to the particles, with the slope

$$\frac{\mathrm{d}x}{\mathrm{d}t} = u - c. \tag{2.12}$$

Here again u, c, and s are continuous across this characteristic.

The interface between the regions C and D is a contact discontinuity and it is a particle path, therefore, the particle velocity must approach the same value as it approached from both sides. The interface moves with finite speed except at $t = 0$; the pressure and particle velocity across it must be continuous. Thus, if $x = x_I(t)$ denotes the contact front, the boundary conditions across it are

$$u_C = u_D, \quad t \ge 0 \quad \text{and} \quad p_C = p_D, \quad t > 0. \tag{2.13}$$

The other variables, namely the density ρ, the sound speed c, and the entropy s must suffer a jump across $x = x_I(t)$.

The shock front moves outward into the air at a variable velocity U. For perfect 'air' with $p = 1, c = 1$ and $u = 0$ (non-dimensional) ahead of the shock, the Rankine–Hugoniot conditions [17] across the shock, $x = x_s(t),\ t > 0$ are

$$u_D = \alpha(U^2 - 1)/(\alpha + 1)U, \tag{2.14}$$

$$c_D^2 = [(\alpha + 2)U^2 - 1](U^2 + \alpha)/(\alpha + 1)^2 U^2, \tag{2.15}$$

$$p_D = [(\alpha + 2)U^2 - 1]/(\alpha + 1), \tag{2.16}$$

where u_D, u_C and p_D are particle velocity, sound velocity and pressure behind the shock front, respectively.

3. Series solution

We introduce the independent variables

$$q = \frac{1}{(\alpha+1)}[\alpha + (1-x)/c_A t] \quad \text{and} \quad y = c_A t. \tag{3.1}$$

into the basic system of Eqs. (2.7)–(2.9).

The flow variables u, c, and s are assumed to be analytic functions of q and y in each of the regions B, C, and D and are expressed in the form of power series

$$u(q,y) = \sum_{n=0}^{\infty} u_n(q) y^n, \qquad c(q,y) = \sum_{n=0}^{\infty} c_n(q) y^n, \qquad s(q,y) = \sum_{n=0}^{\infty} s_n(q) y^n, \tag{3.2}$$

where $u_n(q)$, $c_n(q)$ and $s_n(q)$are assumed to be sufficiently smooth.

Substituting (3.2) into (2.7)–(2.9) after using the transformation (3.1) we find an infinite set of ordinary differential equations in q. The zeroth order equations are

$$(c_A\lambda - u_0)\, u_o' - \alpha c_0 c_0' + c_0^2 s_0' = 0, \tag{3.3}$$

$$-c_0 u_0' + \alpha\,(c_A\lambda - u_0)\, c_0' = 0, \tag{3.4}$$

$$(c_A\lambda - u_0)\, s_0' = 0, \tag{3.5}$$

where the prime denotes differentiation with respect to q.

The nth order $(n \geq 1)$ system is found to be

$$\begin{aligned}
&(c_A\lambda - u_0)\, u_n' + \left(2nNc_A - u_0'\right)\, u_n - \alpha c_0 c_n' + \left(2c_0 s_0' - \alpha c_0'\right)\, c_n + c_0^2 s_n' - \sum_{i=1}^{n-1} u_i' u_{n-i} \\
&\quad + \sum_{i=1}^{n-1} \left(2c_0 s_{n-i}' + 2c_1 s_{n-i-1}' + \alpha s_{n-i}'\right)\, c_i + \sum_{i=1(2i<n)}^{n-1} c_i^2 s_{n-2i}' = 0,
\end{aligned} \tag{3.6}$$

$$\begin{aligned}
&-c_0 u_n' - \alpha c_0' u_n + \alpha\,(c_A\lambda - u_0)\, c_n' + \left\{n c_A\,(\alpha+1)\,\alpha - u_0'\right\}\, c_n - \sum_{i=1}^{n-1}\left(u_i' c_{n-i} + \alpha c_i u_{n-i}\right) \\
&\quad + \sigma\,(\alpha+1) \sum_{j=0}^{n-1} (-1)^j \lambda^j \left(\sum_{i=j}^{n-1} c_{i-j} u_{n-i-1}\right) = 0,
\end{aligned} \tag{3.7}$$

$$(c_A\lambda - u_0)\, s_n' + n c_A\,(\alpha+1)\, s_n - \sum_{i=1}^{n} u_i s_{n-1}' = 0, \tag{3.8}$$

where $\lambda = \alpha - (\alpha+1)q$. The zeroth order system of ODEs is nonlinear while all higher order systems are linear and inhomogeneous.

We must now find the boundary conditions, to different orders, across the interfaces to use them in conjunction with the system (3.3)–(3.5) for $n = 0$ and for (3.6)–(3.8) for $n \geq 1$.

The zeroth order conditions at the head of the rarefaction wave are

$$u_0(1) = 0, \qquad c_0(1) = c_A, \qquad s_0(1) = s_A, \tag{3.9}$$

while, for the higher orders,

$$u_n(1) = 0, \qquad c_n(1) = 0, \qquad s_n(1) = 0, \quad n \geq 1. \tag{3.10}$$

The conditions suffice to uniquely determine the series solution in the region B.

At the tail of the rarefaction wave, contact front and shock, q varies with y. We may write

$$q_T = \sum_{n=0}^{\infty} q_{Tn} y^n, \qquad q_I = \sum_{n=0}^{\infty} q_{In} y^n, \qquad q_s = \sum_{n=0}^{\infty} q_{sn} y^n, \tag{3.11}$$

where q_{T0}, q_{I0}, and q_{s0} are related to the slopes of the respective paths at $t = 0$. The higher coefficients q_{Tn}, q_{In} and q_{sn}, $(n \geq 1)$ must be determined as part of the solution.

Now we derive the boundary conditions across the tail of the rarefaction wave which is a negative characteristic with

$$\frac{\mathrm{d}x_T}{\mathrm{d}t} = u\,(q_T + 0, y) - c\,(q_T + 0, y)\,. \tag{3.12}$$

This equation, in view of definition $q = q_T$ (see (3.1) and (3.11)) and the expansions (3.2), becomes

$$c_A[\alpha-(1+\alpha)q_{T0}]-\sum_{n=1}^{\infty}(n+1)c_A(1+\alpha)q_{Tn}y^n=\sum_{n=0}^{\infty}u_n\left(\sum_{n=0}^{\infty}q_{Tn}y^n\right)y^n-\sum_{n=0}^{\infty}c_n\left(\sum_{n=0}^{\infty}q_{Tn}y^n\right)y^n. \tag{3.13}$$

Equating different powers of y on both sides, we have

$$u_0(q_{T_0})-c_0(q_{T_0})=c_A\{\alpha-(\alpha+1)q_{T_0}\},\qquad s_0(q_{T_0})=s_A, \tag{3.14}$$

$$u_1(q_{T_0})-c_1(q_{T_0})=-c_A(1+\alpha)q_{T_1},\qquad s_1(q_{T_0})=0, \tag{3.15}$$

$$u_2(q_{T_0})-c_2(q_{T_0})=-2c_A(1+\alpha)q_{T_2}-\{u_1'(q_{T_0})-c_1'(q_{T_0})\}q_{T_1},\qquad s_0(q_{T_0})=0,\quad \text{etc.} \tag{3.16}$$

It suffices to consider the continuity of the Riemann invariant $(u+\alpha c)$ across the tail to carry the information from region B to C, thus we have

$$[u+\alpha c](q_T+0)=[u+\alpha c](q_T-0). \tag{3.17}$$

Introducing the expansion (3.2) along the tail $q = q_T$ (see (3.11)) and then using the Taylor series expansion and equating the coefficients of y on both sides, we have

$$[u_0(q_{T_0})-\alpha c_0(q_{T_0})]_{\mathrm{B}}=[u_0(q_{T_0})-\alpha c_0(q_{T_0})]_{\mathrm{C}}, \tag{3.18}$$

$$[u_1(q_{T_0})-\alpha c_1(q_{T_0})]_{\mathrm{B}}=[u_1(q_{T_0})-\alpha c_1(q_{T_0})]_{\mathrm{C}}, \tag{3.19}$$

$$[u_2(q_{T_0})-\alpha c_2(q_{T_0})]_{\mathrm{B}}=[u_2(q_{T_0})-\alpha c_2(q_{T_0})]_{\mathrm{C}}+z_1,\quad \text{etc.}, \tag{3.20}$$

where $z_1=[\{u_1'(q_{T_0})+\alpha c_1'(q_{T_0})\}q_{T_1}]_{\mathrm{C}}-[\{u_1'(q_{T_0})+\alpha c_1'(q_{T_0})\}q_{T_1}]_{\mathrm{B}}$.

Since the contact front is a particle path, we have

$$\frac{\mathrm{d}x_I}{\mathrm{d}t}=u(q_I+0,y). \tag{3.21}$$

We use (3.1) and (3.11) in (3.21) and apply Taylor series expansion and after equating the coefficients of y on both sides, we get

$$u_0(q_{I_0})=c_A[\alpha-(1+\alpha)q_{I_0}], \tag{3.22}$$

$$u_1(q_{I_0})=-2(1+\alpha)c_Aq_{I_1}, \tag{3.23}$$

$$u_2(q_{I_0})=-3(1+\alpha)c_Aq_{I_2}-u_1'(q_{I_0})q_{I_1},\quad \text{etc.} \tag{3.24}$$

At the interface the particle velocity is continuous i.e.,

$$u(q_I+0)=u(q_I-0). \tag{3.25}$$

Using the expansion (3.2) in (3.25) and evaluating them at $q = q_I$ (see (3.11)), we get

$$[u_0(q_{I_0})]_{\mathrm{C}}=[u_0(q_{I_0})]_{\mathrm{D}}, \tag{3.26}$$

$$[u_1(q_{I_0})]_{\mathrm{C}}=[u_1(q_{I_0})]_{\mathrm{D}}, \tag{3.27}$$

$$[u_2(q_{I_0})]_{\mathrm{C}}=[u_2(q_{I_0})]_{\mathrm{D}}+q_{I_1}[\{u_1'(q_{I_0})\}_D-\{u_1'(q_{I_0})\}_{\mathrm{C}}],\quad \text{etc.} \tag{3.28}$$

At the interface we also have

$$p(q_I+0)=p(q_I-0),$$

$$\Rightarrow [c^{\alpha+2}\mathrm{e}^{-\gamma s}](q_I+0)=[c^{\alpha+2}\mathrm{e}^{-\gamma s}](q_I-0). \tag{3.29}$$

Again we apply the expansion (3.2) in (3.29) and proceed in the same manner as discussed earlier. We get

$$[c_0^{\alpha+2}(q_{I_0})\mathrm{e}^{-\gamma s_0}]_{\mathrm{C}}=[c_0^{\alpha+2}(q_{I_0})\mathrm{e}^{-\gamma s_0}]_{\mathrm{D}}, \tag{3.30}$$

$$\left[\frac{c_1(q_{I_0})}{c_Aq_{T_0}}\right]_{\mathrm{C}}=\left[\frac{c_1(q_{I_0})}{c_0}\right]_{\mathrm{D}}, \tag{3.31}$$

$$\left[\frac{c_2(q_{I_0})}{c_Aq_{T_0}}\right]_{\mathrm{C}}=\left[\frac{c_2(q_{I_0})}{c_0}\right]_{\mathrm{D}}+z_2,\quad \text{etc.}, \tag{3.32}$$

where,

$$z_2=\left[\frac{c_1'(q_{I_0})}{c_0}q_{I_1}-\frac{c_1'(q_{I_0})}{c_Aq_{I_0}}q_{I_1}-\frac{\gamma s_2(q_{I_0})}{\alpha+2}\right]_{\mathrm{D}}.$$

Finally, we consider the conditions at the shock front. If the shock U is written as

$$U = \sum_{n=0}^{\infty} U_n y^n \tag{3.33}$$

then we have the shock front locus as

$$\frac{\mathrm{d}x_s}{\mathrm{d}t} = \sum_{n=0}^{\infty} U_n y^n. \tag{3.34}$$

Putting $q = q_s$ and $x = x_s$ in the definition (3.1) of q, we obtain the following relations:

$$U_0 = c_A(\alpha - (1+\alpha)q_{s0}), \quad n = 0, \tag{3.35}$$

$$U_n = -(n+1)(1+\alpha)c_A q_{sn}, \quad n \geq 1. \tag{3.36}$$

Substituting the expressions (3.2) and (3.11) into the Rankine–Hugoniot conditions (2.14)–(2.16) and equating coefficients of equal powers of y on both sides, we get

$$u_{D_0}(q_{s_0}+0) = \frac{\alpha(U_0^2-1)}{(\alpha+1)U_0}, \tag{3.37}$$

$$u_{D_1}(q_{s_0}+0) = \frac{\alpha(U_0^2+1)}{(\alpha+1)U_0^2}U_1, \tag{3.38}$$

$$u_{D_2}(q_{s_0}+0) = \frac{\alpha[(U_0^3+U_0)U_2 - U_1^2]}{(\alpha+1)U_0^3} - u'_{D_1}(q_{s_0})(q_{s_1}), \quad \text{etc.}, \tag{3.39}$$

$$c_{D_0}^2(q_{s_0}+0) = [(\alpha+2)U_0^2 - 1](U_0^2+\alpha)/(\alpha+1)^2U_0^2, \tag{3.40}$$

$$c_{D_1}(q_{s_0}+0) = \frac{\{(\alpha+2)U_0^2+\alpha\}U_1}{(\alpha+1)^2 c_{D_0} U_0^3}, \tag{3.41}$$

$$c_{D_2}(q_{s_0}+0) = \frac{\{(\alpha+2)U_0^4+\alpha\}U_2}{(\alpha+1)^2 c_{D_0} U_0^3} + \frac{\{(\alpha+2)U_0^4 - 3\alpha\}U_1^2}{2(\alpha+1)^2 c_{D_0} U_0^4} - \frac{c_{D_1}^2}{2c_{D_0}} - c'_{D_1} q_{s_0}, \quad \text{etc.}, \tag{3.42}$$

$$c_{D_0}^{2N+1} \mathrm{e}^{-\gamma s_{D_0}} = (\alpha+2)(U_0^2-1)/(\alpha+1), \tag{3.43}$$

$$s_{D_1}(q_{s_0}) = \left\{ \frac{\alpha c_{D_1}}{c_{D_0}} - \frac{2\alpha U_0}{(\alpha+2)U_0^2 - 1} \right\} U_1, \tag{3.44}$$

$$s_{D_2}(q_{s_0}) = z_3 U_2 + z_4, \quad \text{etc.}, \tag{3.45}$$

where

$$z_3 = -\frac{2\alpha U_0}{(\alpha+2)U_0^2 - 1},$$

$$z_4 = -\frac{(\alpha+2)U_1^2}{\gamma\{(\alpha+2)U_0^2-1\}} + \frac{\gamma s_{D_2}^2}{2} - s'_{D_1} q_{s_1} + \frac{(\alpha+2)s_{D_1} c_{D_1}}{c_{D_0}} + \frac{(\alpha+2)(c_{D_2} + c'_{D_1} q_{s_1})}{\gamma c_{D_0}} + \frac{(\alpha+1)(\alpha+2)c_{D_1}^2}{2\gamma c_{D_0}^2}.$$

Now we turn to explicit forms of the solutions for different orders which satisfy appropriate boundary conditions at the boundaries of different regions.

4. Solution in region B

The flow in the rarefaction region B is isentropic. The region is bounded by the head and the tail of rarefaction wave. The zeroth order solution is obtained by solving the system (3.3)–(3.5) with zeroth order boundary conditions (3.9). This solution along with its derivatives is used for obtaining the solutions of the system (3.6)–(3.8) at subsequent orders.

Zeroth order coefficients

The Eq. (3.5) is solved with the boundary condition (3.9) for s_o, which yields $s_o = s_A$. Substituting $s'_o = 0$ in Eqs. (3.3)–(3.4) and combining them suitably, we get

$$[c_A\lambda - (u_0 \pm c_0)][u_0 \pm \alpha c'_0] = 0. \tag{4.1}$$

The system (4.1) has four possible solutions depending on the factors that are set equal to zero. The solutions compatible with the boundary conditions (3.9) are

$$u_o = c_A\alpha(1-q), \tag{4.2}$$

$$c_o = c_A q, \tag{4.3}$$

$$s_o = s_A. \tag{4.4}$$

The solutions (4.2)–(4.4) describing a centered simple rarefaction wave are identical with the solutions of a plane shock tube discussed by Courant and Friedrichs [18].

First order coefficients

Substituting the zeroth order solutions (4.2)–(4.4) and their derivatives in (3.6)–(3.8) with $n = 1$, we get the following inhomogeneous system of ODEs:

$$qu_1' - (4N-1)\,u_1 + \alpha q c_1' + \alpha c_1 + h_o(q) = c_A q^2 s_1', \tag{4.5}$$

$$qu_1' + \alpha u_1 + \alpha q c_1' - \alpha(2N+1)\,c_1 + g_o(q) = 0, \tag{4.6}$$

$$qs_1' - (\alpha+1)\,s_1 = 0, \tag{4.7}$$

where

$$h_o(q) = 0, \qquad g_o(q) = -\frac{2\sigma N u_o c_o}{c_A}.$$

The solutions of the Eqs. (4.5) and (4.6) have different forms depending on the value of N. For $N \neq 1, 2$, we have

$$u_1 = u_{1,1}q + u_{1,2}q^2 + u_{1,1,1}q^N, \tag{4.8}$$

$$c_1 = c_{1,1}q + c_{1,2}q^2 + c_{1,1,1}q^N \quad , \tag{4.9}$$

$$s_1 = 0, \tag{4.10}$$

where

$$u_{1,1} = -\frac{0.5\sigma c_A q_{T_o}}{(N-1)}, \qquad u_{1,2} = -\frac{0.75\sigma c_A q_{T_o}}{(N-2)}, \qquad u_{1,1,1} = -\frac{0.25\sigma c_A q_{T_o}\,(N+1)}{\{(N-1)\,(N-2)\}},$$

$$c_{1,1} = u_{1,1}, \qquad c_{1,2} = -\frac{0.25\sigma c_A\,(4N-3)}{(N-2)}, \qquad c_{1,1,1} = -\frac{0.25\sigma c_A\,(3N-1)}{\{(N-1)\,(N-2)\}},$$

$$q_{T_o} = (2N-1)\,.$$

Second order coefficients

The solutions obtained for zeroth order and first order coefficients, along with their derivatives are substituted in (3.6)–(3.8) with $n = 2$ to have the following system:

$$qu_2' - (6N-1)\,u_2 + \alpha q c_2' + \alpha c_2 + h_1(q) = c_A q^2 s_2', \tag{4.11}$$

$$qu_2' + \alpha u_2 + \alpha q c_2' - \alpha\,(4N+1)\,c_2 + g_1(q) = 0, \tag{4.12}$$

$$qs_2' - 4Ns_2 = 0, \tag{4.13}$$

where

$$h_1(q) = \frac{1}{c_A}[u_1'u_1 + \alpha c_1'c_1],$$

$$g_1(q) = \frac{1}{c_A}[u_1'c_1 + \alpha c_1'u_1 - 2N\sigma\{(u_oc_1 + u_1c_o) - \lambda u_oc_o\}].$$

The above system of ODEs is solved with the boundary conditions (3.10) to find u_2, c_2 and s_2. Again for the same reason stated while finding s_1; s_2 is also equal to zero. We obtain the second order coefficients u_2, c_2 and s_2 of particle velocity, sound speed and entropy as follows:

$$u_2 = u_{2,1}q + u_{2,2}q^2 + u_{2,3}q^3 + u_{2,1,1}q^N + u_{2,1,2}q^{N+1} + u_{2,2,1}q^{2N-1} + u_{2,2,2}q^{2N}, \tag{4.14}$$

$$c_2 = c_{2,1}q + c_{2,2}q^2 + c_{2,3}q^3 + c_{2,1,1}q^N + c_{2,1,2}q^{N+1} + c_{2,2,1}q^{2N-1} + c_{2,2,2}q^{2N}, \tag{4.15}$$

$$s_2 = 0. \tag{4.16}$$

For the coefficients in (4.14)–(4.16) we refer to Haque [10].

5. Solution in region C

Region C is nearly uniform outside the main expansion. This region is bounded by the tail of the rarefaction wave and the contact front. The analytical solutions of various orders of region C are obtained in a manner similar to that of region B. The entropic changes are assumed to be negligible in region C.

Zeroth order coefficients

The boundary conditions at the tail of rarefaction wave require that the zeroth order solutions in region C be constants. Hence, the zeroth order solution in region C will be the same as that in region B at $q = q_{T_0}$, i.e.,

$$u_o = c_A\alpha(1 - q_{T_0}), \qquad c_o = c_A q_{T_0}, \quad \text{and} \quad s_o = s_A. \tag{5.1}$$

First order coefficients

Substituting the zeroth order solution in the system (3.6)–(3.8) with $n = 1$, we have the following system of ODEs:

$$[\alpha q_{T_o} - (\alpha+1)\,q]\,u_1' + (\alpha+1)\,u_1 - \alpha q_{T_o}c_1' + c_A q_{T_o}^2 s_1' - h_o(q_{T_o}) = 0, \tag{5.2}$$

$$-q_{T_o}u_1' + \alpha[\alpha q_{T_o} - (\alpha+1)\,q]\,c_1' + (\alpha+1)\,\alpha\,c_1' - g_o(q_{T_o}) = 0, \tag{5.3}$$

$$[\alpha q_{T_o} - (\alpha+1)\,q]\,s_1' + (\alpha+1)\,s_1' = 0, \tag{5.4}$$

where

$$h_o(q_{T_o}) = 0, \quad g_o(q_{T_o}) = -\sigma\alpha(\alpha+1)\,c_A q_{T_o}(1 - q_{T_o}).$$

We solve (5.2)–(5.4) subject to the boundary condition (3.15), which gives

$$u_1 = u_{1,0} + u_{1,1}q, \tag{5.5}$$

$$c_1 = c_{1,0} + c_{1,1}q, \tag{5.6}$$

$$s_1 = 0, \tag{5.7}$$

where

$$u_{1,0} = \frac{q_{T_o}[(N-1)\,k_{1,1} + Nk_{1,2}]}{2} \qquad u_{1,1} = \frac{-N[k_{1,1} + k_{1,2}]}{2}$$

$$c_{1,0} = \frac{q_{T_o}[(N-1)\,k_{1,1} + Nk_{1,2}]}{2\alpha} - \sigma c_A q_{T_o}(1 - q_{T_o}), \qquad c_{1,1} = \frac{-N[k_{1,1} + k_{1,2}]}{2\alpha}.$$

Second order coefficients

After substituting the zeroth order and first order solutions into (3.6)–(3.8) with $n = 2$, we have the second order ODEs:

$$[\alpha q_{T_o} - (\alpha+1)q]\,u_2' + 4Nu_2 - \alpha q_{T_o}c_2' + c_A q_{T_o}^2 s_2' - h_1(q) = 0, \tag{5.8}$$

$$-q_{T_o}u_2' + \alpha[\alpha q_{T_o} - (\alpha+1)\,q]\,c_2' + 4N\alpha c_2 - g_1(q) = 0, \tag{5.9}$$

$$[\alpha q_{T_o} - (\alpha+1)\,q]\,s_2' + 4Ns_2 = 0. \tag{5.10}$$

The system (5.7)–(5.9), is solved subject to boundary condition (3.16) for the following second order coefficients

$$u_2 = u_{2,0} + u_{2,1}q + u_{2,2}q^2, \tag{5.11}$$

$$c_2 = c_{2,0} + c_{2,1}q + c_{2,2}q^2. \tag{5.12}$$

$$s_2 = 0. \tag{5.13}$$

For the coefficients in (5.11)–(5.13) we refer to Haque [10].

6. Solution in region D

Region D contains compressed air moving outward. The transition from region E to D takes place in the form of a shock. The flow in this region is non-isentropic. The region is bounded by the contact front and shock front. Following the procedure applied to region C, we obtain the analytical solution from zeroth to fourth order. The structure of the nth order solution is discussed at the end of the section.

Zeroth order coefficients

The boundary conditions (2.14)–(2.16) at the shock boundary and the boundary condition (2.13) at the interface require the zeroth order solutions to be constants. These are

$$u_0 = u_{D_0}, \qquad c_0 = c_{D_0}, \qquad s_0 = s_{D_0}. \tag{6.1}$$

The method of evaluation of these constants is given in Section 8.

First order coefficients

Since the zeroth order solutions are constants, their derivatives vanish. Substituting these in (3.6)–(3.8) for $n = 1$, we get the first order ordinary differential equations as

$$(c_A\lambda - u_{D_0})u_1' + 2Nc_Au_1 - \alpha c_{D_0}c_1' + c_{D_0}^2 s_1' + h_0(q) = 0, \tag{6.2}$$

$$-c_{D_0}u_1' + \alpha(c_A\lambda - u_{D_0})c_1' + 2Nc_A\alpha c_1 + g_0(q) = 0, \tag{6.3}$$

$$(c_A\lambda - u_{D_0})s_1' + 2Nc_As_1 + f_0(q) = 0, \tag{6.4}$$

where

$$h_0(q) = 0, \qquad g_0(q) = -2N\sigma\lambda u_{D_0}c_{D_0}, \qquad f_0(q) = 0.$$

The solution of (6.2)–(6.4) is

$$u_1 = u_{1,0} + u_{1,1}q, \tag{6.5}$$

$$c_1 = c_{1,0} + c_{1,1}q, \tag{6.6}$$

$$s_1 = s_{1,0} + s_{1,1}q. \tag{6.7}$$

The coefficients in (6.5)–(6.7) are given by

$$u_{1,0} = \frac{(K_{1,1}p_1 + K_{1,2}p_2)}{2} + c_{D0}^2K_{1,3}, \qquad u_{1,1} = -c_AN(K_{1,1} + K_{1,2}),$$

$$c_{1,0} = \frac{(K_{1,1}p_1 - K_{1,2}p_2)}{2\alpha} - \frac{\sigma u_{D0}c_{D0}}{c_A\alpha}, \qquad c_{1,1} = \frac{-c_AN(K_{1,1} + K_{1,2})}{\alpha},$$

$$s_{1,0} = 2Nc_Aq_{T_o}K_{1,3}, \qquad S_{1,1} = -2Nc_AK_{1,3},$$

where

$$p_1 = 2Nc_Aq_{T_o} - c_{D0}, \qquad p_2 = 2Nc_Aq_{T_o} + c_{D0}.$$

Second order coefficients

By following a similar procedure, we obtain the ordinary differential equations for the second order coefficients of particle velocity, sound speed and entropy. These are

$$(c_A\lambda - u_{D_0})u_2' + 4Nc_Au_2 - \alpha c_{D_0}c_2' + c_{D_0}^2 s_2' + 2c_{D_0}s_1'c_1 + h_1(q) = 0, \tag{6.8}$$

$$-c_{D_0}u_2' + \alpha(c_A\lambda - u_{D_0})c_2' + 4Nc_A\alpha c_2 + g_1(q) = 0, \tag{6.9}$$

$$(c_A\lambda - u_{D_0})s_2' + 4Nc_As_2 + f_1(q) = 0, \tag{6.10}$$

where

$$h_1(q) = u_1u_1' + \alpha c_1c_1', \qquad f_1(q) = u_1s_1',$$

$$g_1(q) = c_1u_1' + \alpha c_1u_1' - 2N\sigma\left[(u_0c_1 + u_1c_0) - \lambda u_0c_0\right].$$

The second order solutions of u_2, c_2 and s_2 in the region D are obtained using a similar procedure mentioned for region C and are given by

$$u_2 = u_{2,0} + u_{2,1}q + u_{2,2}q^2, \tag{6.11}$$

$$c_2 = c_{2,0} + c_{2,1}q + c_{2,2}q^2, \tag{6.12}$$

$$s_2 = s_{2,0} + s_{2,1}q + s_{2,2}q^2. \tag{6.13}$$

For the coefficients in (6.11)–(6.13) we refer to Haque [10].

7. Solutions in region B for $\gamma = 5/3, 3$

It can be observed that the coefficients in the first order, solution (4.8)–(4.9) in region B, contains $(N - 1)$ and $(N - 2)$ in the denominator. For $\gamma = 5/3$ and $3N$ becomes 2 and 1 respectively, thus the solution becomes indeterminate for these special values of γ. The solutions for these cases are listed below:

Case 1. $r = 5/3$

Zeroth order coefficients

$$u_0 = c_A\alpha(1 - q), \qquad c_0 = c_Aq. \tag{7.1}$$

First order coefficients

$$u_1 = u_{1,1}q + u_{1,2}q^2 + (q\ln(q))(u_{1,1,1}q), \tag{7.2}$$

$$c_1 = c_{1,1}q + c_{1,2}q^2 + (q\ln(q))(c_{1,1,1}q). \tag{7.3}$$

Second order coefficients

$$u_2 = u_{2,1}q + u_{2,2}q^2 + u_{2,3}q^3 + u_{2,4}q^4 + (q\ln(q))(u_{2,1,1}q + u_{2,1,2}q^2) + (q\ln(q))^2(u_{2,2,1}q), \tag{7.4}$$

$$c_2 = c_{2,1}q + c_{2,2}q^2 + c_{2,3}q^3 + c_{2,4}q^4 + (q\ln(q))(c_{2,1,1}q + c_{2,1,2}q^2) + (q\ln(q))^2(c_{2,2,1}q). \tag{7.5}$$

Case 2. $r = 3$

Zeroth order coefficients

$$u_0 = c_A\alpha(1-q), \qquad c_0 = c_A q. \tag{7.6}$$

First order coefficients

$$u_1 = u_{1,1}q + u_{1,2}q^2 + \ln(q)(u_{1,1,1}q), \tag{7.7}$$

$$c_1 = c_{1,1}q + c_{1,2}q^2 + \ln(q)(c_{1,1,1}q). \tag{7.8}$$

Second order coefficients

$$u_2 = u_{2,1}q + u_{2,2}q^2 + u_{2,3}q^3 + \ln(q)(u_{2,1,1}q + u_{2,1,2}q^2) + (\ln(q))^2(u_{2,2,1}q + u_{2,2,2}q^2), \tag{7.9}$$

$$c_2 = c_{2,1}q + c_{2,2}q^2 + c_{2,3}q^3 + \ln(q)(c_{2,1,1}q + c_{2,1,2}q^2) + (\ln(q))^2(c_{2,2,1}q + c_{2,2,2}q^2). \tag{7.10}$$

For the coefficients in (7.2)–(7.5), (7.7)–(7.10) we refer to Haque [10].

8. Determination of boundaries of regions B, C, D and evaluation of the integrating constants

To find the boundaries; tail of the rarefaction wave, contact front and the shock, and to evaluate the constants of integration for the solutions of regions C and D we use the boundary conditions (3.9)–(3.45) order by order. In the process we use the following main conditions:

(i) The continuity of Riemann invariant at the tail of the rarefaction wave,
(ii) The continuity of the pressure and particle velocity at the contact front, and
(iii) The Rankine–Hugoniot (R–H) conditions at the shock.

Zeroth order

If we equate the zeroth order particle velocity (5.1) of region C with the zeroth order particle velocity (6.1) of region D at the contact front, we get

$$u_{D0} = c_A\alpha(1-q_{T_0}). \tag{8.1}$$

Also using the continuity of pressure across the contact front we get (see Eqs. (2.6), (5.1) and (6.1))

$$c_{D0}^{\alpha+2}e^{-\gamma s_{D0}} = (c_A q_{T_0})^{\alpha+2}e^{-\gamma s_A}. \tag{8.2}$$

From (3.37), (3.40) and (3.43) we have the zeroth order R–H conditions at the shock front as

$$u_{D0} = \frac{\alpha(U_0^2-1)}{(\alpha+1)U_0}, \tag{8.3}$$

$$c_{D_0}^2 = [(\alpha+2)U_0^2 - 1](U_0^2+\alpha)/(\alpha+1)^2U_0^2, \tag{8.4}$$

$$p_{D_0} = c_{D_0}^{\alpha+2}e^{-\gamma s D_0} = (\alpha+2)(U_0^2-1)/(\alpha+1). \tag{8.5}$$

Eqs. (8.1)–(8.5) are solved to get the constants, u_{D_0}, c_{D_0}, S_{D_0}, q_{T_0} and U_0. This involves the solution of equation

$$c_A\alpha(1-q_{T_0}) = \frac{1}{\sqrt{\alpha/2}}\frac{(p_A q_{T_0}^{\alpha+2}-1)}{\sqrt{(\alpha+1)p_A q_{T_0}^{\alpha+2}+1}}, \tag{8.6}$$

for q_{T_0}, where $p_A = c_A^{\alpha+2}e^{-\gamma s_A}$ the initial gas pressure in region A. The other four constants have been computed from the remaining Eqs. (8.1)–(8.5).

From Eqs. (8.1) and (3.22) we have

$$q_{I_0} = \alpha q_{T_0}/(\alpha+1). \tag{8.7}$$

Also from (3.35) we get

$$q_{s_0} = (\alpha - U_0/C_A)/(\alpha+1). \tag{8.8}$$

Hence, all the zeroth order constants are known.

First order

Now we obtain the integrating constants $k_{1,1}, k_{1,2}$, in solutions (5.5)–(5.6) of region C and $K_{1,1}, K_{1,2}, K_{1,3}$, in solutions (6.5)–(6.7) of region D, in the following steps.

(i) We use (4.8)–(4.9) and (5.5)–(5.6) in the continuity of Riemann invariant at the tail of the rarefaction wave i.e., in (3.19) to obtain $k_{1,1}$ as

$$k_{1,1} = -[\{u_1(q_{T_0}) + \alpha c_1(q_{T_0})\}_{\mathrm{B}} + \alpha c_A \sigma(q_{T_0})(1-q_{T_0})]/(q_{T_0}). \tag{8.9}$$

(ii) From (3.38), (3.41) and (3.44) we have the first order R–H condition at the shock front as

$$u_{D_1}(q_{s_0}) = z_5 U_1, \tag{8.10}$$

$$c_{D_1}(q_{s_0}) = z_6 U_1, \tag{8.11}$$

$$s_{D_1}(q_{s_0}) = z_7 U_1. \tag{8.12}$$

We equate (6.7) and (8.12) to get

$$K_{1,3} = z_8 U_1. \tag{8.13}$$

(iii) Substituting (6.5) and (6.6) in the linear combination $(u_1 + \alpha c_1)_D$ and equating with the linear combination $(u_1+\alpha c_1)$ obtained from (8.10)–(8.11), we get,

$$K_{1,1} = z_9 U_1 + z_{10}. \tag{8.14}$$

(iv) Now if we consider the linear combination $(u_1 - \alpha c_1)$ we get,

$$K_{1,2} = z_{11} U_1 + z_{12}. \tag{8.15}$$

(v) At the interface the particle velocity is continuous. We use (5.5) and (6.5) in (3.27) to get,

$$K_{1,2} = z_{13} U_1 + z_{14}. \tag{8.16}$$

(vi) At the interface the pressure is also continuous. We use (5.6) and (6.6) in (3.31) to get

$$U_1 = z_{15}/z_{16}. \tag{8.17}$$

Now we use (8.17) in (8.13)–(8.16) to get $k_{1,2}, K_{1,1}, K_{1,2}$, and $K_{1,3}$. Hence the first order coefficients u_1, c_1 and s_1 in (3.2) in all the regions are obtained. The quantities q_{T_1}, q_{I_1} and q_{s_1} can be obtained from (3.15), (3.23) and (3.36). Where $z_5 - z_{16}$ are

$$z_5 = \frac{\alpha(U_0^2+1)}{(\alpha+1)U_0^2}, \qquad z_6 = \frac{(\alpha+2)U_0^4+\alpha}{(\alpha+1)^2 c_{D0} U_0^3}, \qquad z_7 = \frac{\alpha c_{D1}}{c_{D0}} - \frac{2\alpha U_0}{(\alpha+2)U_0^2-1},$$

$$z_8 = \frac{z_7}{(\alpha+1)c_A(q_{I0}-q_s)},$$

$$z_9 = \frac{\alpha(U_0^2+1)/(\alpha+1)U_0^2 + \{\alpha(\alpha+2)U_0^4+\alpha\}/\{(\alpha+1)^2 c_{D0}U_0^3\} - c_{D0}^2 z_8}{\{p_1 - (\alpha+1)c_A q_{s0}\}},$$

$$z_{10} = \sigma U_{D0} c_{D0}/\{c_A(p_1 - (\alpha+1)q_{s0})\},$$

$$z_{11} = \frac{\alpha(U_0^2+1)/(\alpha+1)U_0^2 + \{\alpha(\alpha+2)U_0^4+\alpha\}/\{(\alpha+1)^2 c_{D0}U_0^3\} - c_{D0}^2 z_8}{\{p_2 - (\alpha+1)c_A q_{s0}\}},$$

$$z_{12} = -z_{10}, \qquad z_{13} = \frac{4}{q_{I0}}\left\{-\frac{c_{D0}}{2}(z_9 - z_{11}) + c_{D0}^2 z_8\right\}, \qquad z_{14} = k_{1,1} - \frac{2c_{D0}}{q_{T0}}(z_{10}-z_{12}),$$

$$z_{15} = \frac{\sigma(1-q_{T0}) - \sigma U_{D0}}{\{\alpha c_A + (z_{14}+k_{1,1})\}/4\alpha c_A}, \qquad z_{16} = \frac{(z_9+z_{11})}{(2\alpha - z_{13})/4\alpha c_A}.$$

Second order

To obtain the integrating constants $k_{2,1}, k_{2,2}$, in solutions (5.11)–(5.12) of region C and $K_{2,1}, K_{2,2}, K_{2,3}$, in solutions (6.11)–(6.13) of region D, we proceed as for the first order.

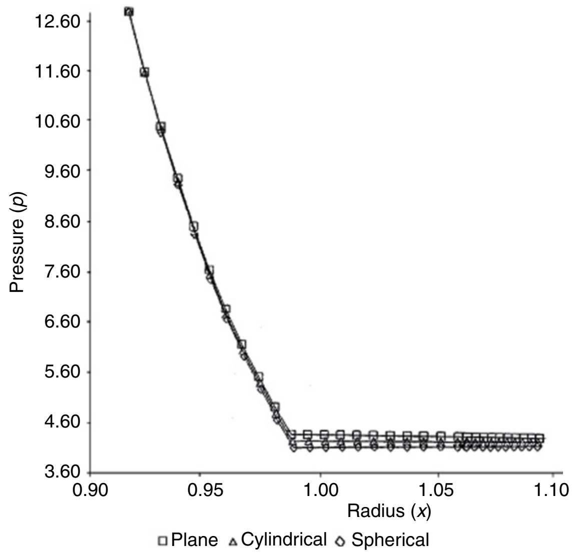

Fig. 2. Pressure distribution in the entire disturbed region behind the shock: $\gamma = 7/5$, $c_A = 1.8$, $p_A = 12.818$, $t = 0.05$ and $\sigma = 2$.

(i) We use (4.14)–(4.15) and (5.11)–(5.12) in the continuity of Riemann invariant at the tail of the rarefaction wave i.e., in (3.20) to obtain $k_{2,1}$ as

$$k_{2,1} = -[\{u_2(q_{T_o}) + \alpha c_2(q_{T_o}).\}_B - z_{17}]/q_{T_o}^2. \tag{8.18}$$

(ii) From (3.39), (3.42) and (3.5) we have the first order R–H condition at the shock front as

$$u_2(q_{s_0}) = z_{18}U_2 + z_{19}, \tag{8.19}$$

$$c_2(q_{s_0}) = z_{20}U_2 + z_{21}, \tag{8.20}$$

$$s_2(q_{s_0}) = z_{22}U_2 + z_{23}. \tag{8.21}$$

We equate (6.13) and (8.21) to get

$$K_{2,3} = z_{24}U_2 + z_{25}. \tag{8.22}$$

(iii) Substituting (6.11)–(6.12) in the linear combination $(u_1 + \alpha c_1)_D$ and equating with the linear combination $(u_1 + \alpha c_1)$ obtained from (8.19)–(8.20), we get,

$$K_{2,1} = z_{26}U_2 + z_{27}. \tag{8.23}$$

(iv) Now if we consider the linear combination $(u_1 - \alpha c_1)$ we get,

$$K_{2,2} = z_{28}U_2 + z_{29}. \tag{8.24}$$

(v) At the interface the particle velocity is continuous. We use (5.11) and (6.11) in (3.28) to get,

$$k_{2,2} = z_{30}U_2 + z_{31}. \tag{8.25}$$

(vi) At the interface the pressure is also continuous. We use (5.12) and (6.12) in (3.32)

$$U_2 = z_{32}/z_{33}. \tag{8.26}$$

Now we use (8.26) in (8.22)–(8.25) to get $k_{2,2}$, $K_{2,1}$, $K_{2,2}$, and $K_{2,3}$. Hence the first order coefficients u_2, c_2 and s_2 in (3.2) in all the regions are obtained. The quantities q_{T_2}, q_{I_2} and q_{s_2} can be obtained from (3.16), (3.24) and (3.36). We refer [10] for $z_{17} - z_{33}$.

The above procedure can be systematized as an algorithm [10] to find higher order terms in the series solution (3.2). As may be observed, the higher order coefficients in the series (3.2) and (3.11) become rather unwieldy. We therefore do not give explicit results for higher order terms. The task of generating higher order terms satisfying appropriate boundary conditions in each of the regions was delegated to the computer. Twenty terms were generated in each of the regions, and summed directly and by the use of Padé summation.

9. Results and discussion

We consider here an example for a spherical blast. Consider a diatomic gas ($\gamma = 1.4$) contained in a sphere of unit (non-dimensional) radius surrounded by diatomic air. Let initial pressure ratio p_A be 12.818, and the initial sound speed c_A be 1.8.

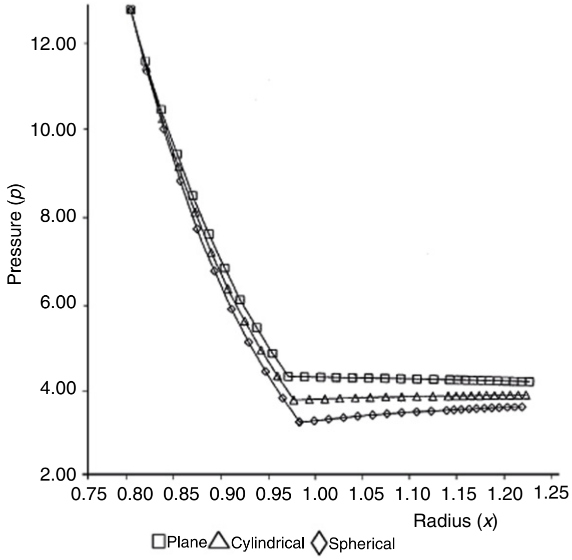

Fig. 3. Pressure distribution in the entire disturbed region behind the shock: $\gamma = 7/5$, $c_A = 1.8$, $p_A = 12.818$, $t = 0.20$ and $\sigma = 2$.

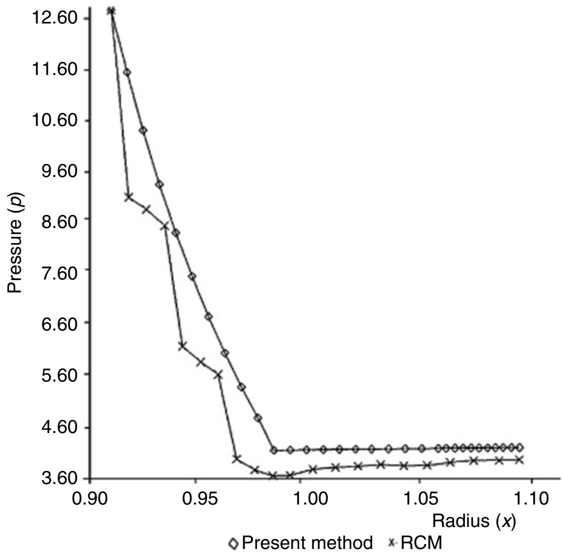

Fig. 4. Comparison of distribution obtained by RCM and the present method: $\gamma = 7/5$, $c_A = 1.8$, $p_A = 12.818$, $t = 0.05$ and $\sigma = 2$.

We use the first five coefficients in the series solution (3.2) to obtain the flow variables pressure p, density ρ, particle velocity u, sound speed c and entropy s in regions B, C, and D. The coefficients of the series (3.11), namely, q_{T_i}, q_{I_i} and q_{s_i} $(i = 0, 1, 2, 3, 4)$, that determine the loci of the tail of the rarefaction wave, contact front, and the shock front, respectively, and the coefficients U_i $(i = 0, 1, 2, 3, 4)$ of the series (3.33) which determine the velocity of the main shock are calculated. The pressure–distance curves for the entire disturbed region behind the main shock are given in Figs. 2–3 for $\gamma = 7/5$, $c_A = 1.8$, $p_A = 12.818$, $t = 0.05$ and $\gamma = 7/5$, $c_A = 1.8$, $p_A = 12.818$, $t = 0.20$ respectively. For comparison the pressure curves for the three geometries – planar, cylindrical and spherical – are plotted in the same figure. The comparison between the pressure curves obtained by Random Choice Method (RCM) [19] and by the present approach for the spherical geometry are given in Fig. 4. While the trend is similar, RCM gives a rather ragged behavior for the pressure curve behind the shock.

The pressure and density distribution behind the main shock at $t = 0.05$ are given in Table 1. It is observed that the pressure p monotonically decreases in region B from 12.818 at $x = 0.91$, the head of the rarefaction wave to 3.9587 at $x = 0.9887$, the tail of the rarefaction wave. Thereafter the pressure monotonically increases in region C from 3.9587 at the tail of the rarefaction wave to 4.0645 at $x = 1.0629$ (the contact front) and continues to increase until it becomes 4.1221 at $x = 1.0993$, the shock front. It may be noted from Table 1 that the density ρ monotonically decreases in region B from 5.5386 at the head of the rarefaction wave to 2.4521 at the tail of the rarefaction wave. Then it monotonically increases

Table 1
Pressure and density distribution in the entire disturbed region behind the shock: $\gamma = 1.4$, $c_A = 1.8$, $t = 0.05$, $p_A = 12.818$ and $\sigma = 2$.

q	x	Pressure	Density
Region B			
1.0000	0.9100	12.818	5.5386
0.9854	0.9179	11.515	5.1273
0.9563	0.9336	0.9122	4.2737
0.9271	0.9494	7.3125	3.7090
0.8979	0.9651	5.6551	3.1050
0.8834	0.9730	5.0015	2.7516
0.8688	0.9825	4.4520	2.6069
0.8542	0.9887	3.9587	2.4521
Region C			
0.8542	0.9887	3.9587	2.4521
0.8267	1.0036	3.9640	2.3975
0.7993	1.0184	3.9925	2.4150
0.7718	1.0332	4.0212	2.4225
0.7581	1.0406	4.0305	2.4275
0.7443	1.0481	4.0425	2.4310
0.7306	1.0555	4.0575	2.4350
0.7169	1.0629	4.0645	2.4375
Region D			
0.7169	1.0629	4.0645	3.4279
0.7036	1.0702	4.0750	3.4375
0.6966	1.0738	4.0825	3.4450
0.6831	1.0811	4.0923	3.4595
0.6764	1.0848	4.1010	3.4660
0.6629	1.0920	4.1115	3.4785
0.6561	1.0957	4.1168	3.4897
0.6494	1.0993	4.1221	3.5051

Table 2
Time to which the direct series solution is valid at the boundaries ($p_A = 12.818$).

γ	c_A	x_H	x_T	x_I	x_S
$\sigma = 1$					
1.200	1.800	0.55*	3.7	0.50	0.2
1.400	1.800	0.55*	2.6	0.70	0.3
1.800	1.800	0.55*	0.9*	1.30	0.5
1.667	2.417	0.41*	1.1	0.60	0.3
3.000	7.150	0.12*	0.18*	0.62	0.3
$\sigma = 2$					
1.200	1.800	0.55*	2.5	0.50	0.2
1.400	1.800	0.55*	1.8	0.50	0.3
1.800	1.800	0.55*	0.9*	1.10	0.4
1.667	2.417	0.41*	0.71	0.50	0.3
3.000	7.150	0.12*	0.18*	0.42	0.2

* Note: * indicates that the front has reached the center by this time.

in region C from 2.4521 at the tail of the rarefaction wave to 2.4375 at the contact front. At this point density suffers a jump from 2.4375 to 3.4279, and continues to increase thereafter, till it becomes 3.5012 at the shock front. The qualitative behavior of the pressure and density as observed from the Table 1 is similar to that obtained by Saito and Glass [19].

The time $t < 1/c_A$ to which the direct series solution gives reasonable results is given in Table 2 for different values of γ for $\sigma = 1, 2$. The time of validity of the direct series solution in each of the domains B, C and D is different; it also depends on γ and the geometry of the flow. This is clear from Table 2. For example, for $\gamma = 1.4$, the direct series solution breaks down at $t \approx 0.3$ just behind the main shock. This time is even less ($\approx$0.2) for $\gamma = 1.2$.

We observe from Table 2 that the direct series solution holds good for very small time. We generated 20 terms in the series solution and used Padé summation to obtain the solution for larger time. The results were obtained by direct summation and by the use of Padé summation for $t = 0.05, 0.10, 0.20, 0.30, 0.40, 0.50,$ and 0.55, respectively, for the parametric values $\gamma = 7/5, c_A = 1.8, p_A = 12.818$ (Table 3). These are the same initial conditions as were used by McFadden [8]. The direct series sum and the Padé sum agree very well for $t \leq 0.2$, they begin to diverge thereafter. Padé summation extends the validity of the series solution right to the neighborhood of $t = 1/c_A$, the time up to which the present analysis holds (Table 4). Padé summation greatly enhances the time of validity of direct series solution. The present series solution is significantly different from the first order solution of McFadden [8].

Table 3
Flow variables u, c and s in the entire disturbed region: $\gamma = 1.4$, $c_A = 1.8$, $p_A = 12.818$ and $\sigma = 2$.

X	u (direct series)	u (Padé)	c (direct series)	c (Padé)	s (direct series)	s (Padé)
$t = 0.05$						
0.910	0.0000000	0.0000000	1.8000000	1.8000000	1.1169000	1.1169000
0.948	0.6585561	0.6585564	1.6658235	1.6658231	1.1169000	1.1169000
0.986	1.3518029	1.3518082	1.5209044	1.5209033	1.1169000	1.1169000
1.025	1.2945802	1.2945802	1.5247271	1.5247271	1.1169000	1.1169000
1.056	1.2544939	1.2544934	1.5271303	1.5271414	1.1169000	1.1169000
1.075	1.2320518	1.2320510	1.2879540	1.2879535	0.2602136	0.2602135
1.090	1.2153088	1.2153088	1.2862491	1.2862497	0.2495632	0.2495631
1.101	1.2032490	1.2033926	1.2851170	1.2851293	0.2423879	0.2423975
$t = 0.10$						
0.820	0.0000000	0.0000000	1.8000000	1.8000000	1.1169000	1.1169000
0.850	0.2776698	0.2776932	1.7435046	1.7434951	1.1169000	1.1169000
0.911	0.8166859	0.8167043	1.6291137	1.6291061	1.1169000	1.1169000
0.957	1.2096593	1.2096594	1.5426912	1.5426896	1.1169000	1.1169000
1.003	1.3873358	1.3873458	1.4978296	1.4978269	1.1169000	1.1169000
1.050	1.3137040	1.3137040	1.5039347	1.5039347	1.1169000	1.1169000
1.112	1.2341300	1.2341146	1.5097596	1.5098048	1.1169000	1.1169000
1.202	1.1440733	1.1446517	1.2677914	1.2679598	0.2195601	0.2197673
$t = 0.20$						
0.640	0.0000000	0.0000000	1.8000000	1.8000000	1.1169000	1.1169000
0.701	0.3079755	0.3085171	1.7359275	1.7357108	1.1169000	1.1169000
0.823	0.8769163	0.8770572	1.6066419	1.6064606	1.1169000	1.1169000
0.945	1.4043274	1.4043321	1.4784361	1.4784157	1.1169000	1.1169000
0.976	1.5900047	1.5915062	1.4346184	1.4342872	1.1169000	1.1169000
1.223	1.1831536	1.1827123	1.4785606	1.4790494	1.1169000	1.1169000
1.299	1.1187575	1.1180630	1.2429835	1.2415475	0.2277071	0.2275878
1.404	1.0400540	1.0461038	1.2376122	1.2398903	0.1809148	0.1846066
$t = 0.30$						
0.460	0.0000000	0.0000000	1.8000000	1.8000000	1.1169000	1.1169000
0.506	0.1785238	0.1816775	1.7630171	1.7621191	1.1169000	1.1169000
0.734	0.9433479	0.9439845	1.5792530	1.5780814	1.1169000	1.1169000
0.917	1.4655432	1.4655790	1.4392376	1.4390928	1.1169000	1.1169000
0.964	1.8086788	1.8204484	1.3602949	1.3578234	1.1169000	1.1169000
1.335	1.1257709	1.1227931	1.4504838	1.4525959	1.1169000	1.1169000
1.493	1.0278784	1.0260204	1.2159108	1.2178775	0.1977562	0.1940189
1.606	0.9412035	0.9666028	1.2077573	1.2179125	0.1404392	0.1585661
$t = 0.40$						
0.280	0.0000000	0.0000000	1.8000000	1.8000000	1.1169000	1.1169000
0.524	0.7278574	0.7345359	1.6276119	1.6209581	1.1169000	1.1169000
0.890	1.5218926	1.5220456	1.3957038	1.3951239	1.1169000	1.1169000
0.951	2.0849522	2.1385214	1.2690162	1.2584034	1.1169000	1.1169000
1.322	1.1536268	1.1520455	1.4131791	1.4137630	1.1169000	1.1169000
1.446	1.0706920	1.0595710	1.4236080	1.4296007	1.1169000	1.1169000
1.568	1.0213147	1.0021771	1.1855916	1.2396609	0.1860647	0.1860085
1.688	0.9590138	0.9577411	1.1925730	1.1976584	0.1949890	0.1826310
1.808	0.8317933	0.9011115	1.1714605	1.2002374	0.0847204	0.1385084
$t = 0.50$						
0.100	0.0000000	0.0000000	1.8000000	1.8000000	1.1169000	1.1169000
0.557	1.0974655	1.1023752	1.5059920	1.4924473	1.1169000	1.1169000
0.862	1.5727060	1.5731722	1.3472910	1.3455845	1.1169000	1.1169000
0.939	2.4326909	2.6196029	1.15738138	1.1230823	1.1169000	1.1169000
1.171	1.4494802	1.4494759	1.3237928	1.3237125	1.1169000	1.1169000
1.635	1.0133431	0.9690483	1.3958549	1.4179548	1.1169000	1.1169000
1.672	1.0085889	0.9593777	1.1502130	1.2235033	0.1542129	0.1627147
1.972	0.7699870	0.8488669	1.1457286	1.1839538	0.1068825	0.1339416
2.010	0.6920950	0.8462266	1.1219557	1.1857142	0.0003455	0.1225851

Table 3 (*continued*)

X	u (direct series)	u (Padé)	c (direct series)	c (Padé)	s (direct series)	s (Padé)
$t = 0.55$						
0.010	0.0000000	0.0000000	1.8000000	1.8000000	1.1169000	1.1169000
0.513	1.1409062	1.1482120	1.4831459	1.4611208	1.1169000	1.1169000
0.848	1.5958252	1.5965771	1.3210851	1.3183729	1.1169000	1.1169000
0.933	2.6376928	2.9688800	1.0928677	1.0350874	1.1169000	1.1169000
1.358	1.1223364	1.1214092	1.3609618	1.3611854	1.1169000	1.1169000
1.698	1.0089655	0.9423509	1.3790725	1.5096966	1.1169000	1.1169000
1.781	1.0050046	0.9287062	1.1311199	1.1974770	0.1399143	0.1396502
2.028	0.7964193	0.8288778	1.1431177	1.1760787	0.1790078	0.1790276
2.111	0.6069102	0.8219877	1.0901358	1.1793823	−0.0567795	0.1157941

Table 4
Time to which the direct series solution and Padé summation are valid at the boundaries ($P_A = 12.818$).

γ	c_A	x_H	x_T	x_I	x_S
$\sigma = 1$					
1.200	1.800	0.55[a] (0.55)	3.7 (4.1[a])	0.50 (5.0[b])	0.2 (5.0[b])
1.400	1.800	0.55[a] (0.55)	2.6 (3.6[a])	0.70 (5.0[b])	0.3 (5.0[b])
1.800	1.800	0.55[a] (0.55)	0.9[a] (0.9)	1.30 (5.0[b])	0.5 (5.0[b])
1.667	2.417	0.41[a] (0.41)	1.1 (2.1[a])	0.60 (5.0[b])	0.3 (5.0[b])
3.000	7.150	0.12[a] (0.12)	0.18[a] (0.18)	0.62 (0.62[a])	0.3 (2.5[b])
$\sigma = 2$					
1.200	1.800	0.55[a] (0.55)	2.5 (5.0[b])	0.50 (5.0[b])	0.2 (5.0[b])
1.400	1.800	0.55[a] (0.55)	1.8 (3.6[a])	0.50 (5.0[b])	0.3 (5.0[b])
1.800	1.800	0.55[a] (0.55)	0.9[a] (0.9)	1.10 (1.6)	0.4 (2.0)
1.667	2.417	0.41[a] (0.41)	0.71 (2.1[a])	0.50 (5.0[b])	0.3 (5.0[b])
3.000	7.150	0.12[a] (0.12)	0.18[a] (0.18)	0.42 (0.42)	0.2 (5.0[b])

Numbers in the brackets show the time to which Padé approximation gives a converged solution at the boundaries.
[a] Indicates that the front reaches slightly beyond the center by this time.
[b] Indicates that the results are valid beyond this time.

Acknowledgement

P.L. Sachdev, co-author of this paper recently passed away. We sincerely acknowledge his contribution to preparing this paper.

References

[1] G.I. Taylor, The formation of a blast wave by a very intense explosion, Proc. Roy. Soc. A 201 (1950) 159.
[2] L.I. Sedov, Propagation of intense blast waves, Prikl. Mat. Mech. 10 (1946) 241.
[3] L.I. Sedov, Similarity and Dimensional Methods in Mechanics, Academic Press, New York, 1959.
[4] J. Von Neumann, The point source solution, National Defence Research Committee, Division B, Rept.AM9, 1941.
[5] J. Von Neumann, Progress report on the theory of shock waves, National Defence Research Committee, Division B, OSRD No. 1140, 1943.
[6] J. Von Neumann, Blast wave calculation, Comput. Appl. Math. 8 (1955) 327.
[7] M.P. Friedman, A simplified analysis of spherical or cylindrical blast waves, J. Fluid Mech. 11 (1961) 1.
[8] J.A. McFadden, Initial behaviour of a spherical blast, J. Appl. Phys. 3 (1952) 362.
[9] A.M.N. Yogi, On the analytic theory of explosions, Ph.D. thesis, Indian Institute of Science, Bangalore, 1995.
[10] M.E. Haque, Exact analytic solutions of compressible flow equations with applications to explosions, Ph.D. Thesis, Bangalore University, Bangalore, 2002.
[11] P.L. Sachdev, Shock Waves and Explosions, Chapman & Hall/CRC Press, London, 2004.
[12] C.M. Bender, S.A. Orszag, Advanced Mathematical Methods for Scientists and Engineers, McGraw-Hill, New York, 1978.
[13] M. Van Dyke, Analysis and improvement of perturbation series, Quart. J. Mech. Appl. Math. 27 (1974) 423.
[14] M. Van Dyke, Computer extension of perturbation series in fluid mechanics, SIAM J. Appl. Math. 28 (1975) 720.
[15] M. Van Dyke, A.J. Guttmann, The converging shock wave from a spherical or cylindrical piston, J. Fluid Mech. 120 (1982) 451.
[16] M. Van Dyke, Computer-extended series, Ann. Rev. Fluid Mech. 16 (1984) 287.
[17] G.B. Whitham, Linear and Nonlinear Waves, John Wiley & Sons, New York, 1974.
[18] R. Courant, K.O. Friedrichs, Supersonic Flow and Shock Waves, Interscience Publishers Inc, New York, 1948.
[19] T. Saito, I.I. Glass, Applications of random-choice method to problems in shock and detonation-wave dynamics. UTIAS Report. No. 240, 1979.